

Probing Robust Majorana Signatures by Crossed Andreev Reflection with a Quantum Dot

Guan-Hao Feng and Hong-Hao Zhang*

School of Physics, Sun Yat-sen University, Guangzhou 510275, China

We propose a three-terminal structure to probe robust signatures of Majorana zero modes. This structure consists of a quantum dot coupled to the normal metal, s-wave superconducting and Majorana Y-junction leads. The zero-bias differential conductance at zero temperature of the normal-metal lead peaks at $2e^2/h$, which will be deflected after Majorana braiding. This quantized conductance can entirely arise from the Majorana-induced crossed Andreev reflection, protected by the energy gap of the superconducting lead. We find that the effect of thermal broadening is significantly suppressed when the dot is on resonance. In the case that the energy level of the quantum dot is much larger than the superconducting gap, tunneling processes are dominated by Majorana-induced crossed Andreev reflection. Particularly, a novel kind of crossed Andreev reflection equivalent to the splitting of charge quanta $3e$ occurs after Majorana braiding.

I. INTRODUCTION

Majorana zero modes (MZMs) are zero-energy quasi-particle excitations originating from coherent superpositions of electrons and holes. Following theoretical suggestions, MZMs are supported in 1D systems, such as InAs or InSb wires with strong spin-orbit and proximity-induced couplings [1, 2], and they show great potential in decoherence-free quantum computation [3–6]. Verifying the existence of MZMs and their non-Abelian braiding has been attracting much attention in recent years [7–16].

Due to the property that an MZM can act as both an electron lead and a hole lead in tunneling processes, one of the most exciting theoretical predictions is a quantized zero-bias conductance peak (ZBCP) of $\frac{2e^2}{h}$ at zero temperature [17–19]. However, it is quite difficult to observe this quantization from a direct junction between a normal-metal lead and MZMs in a single-subband wire because of thermal broadening, overlap of Majorana wave functions, disorder, and localized Andreev bound states [8, 20–25]. Although the observation of ZBCP has been reported in many experiments in recent years [26–30], the observation of MZMs has not been fully confirmed. Importantly, very recently it has been recognized that one needs to be cautious about the interpretation of non-quantized ZBCP as the signature of MZMs in local tunneling experiments since such experiments only measure one end of the one-dimensional setup [31], while the most important characteristics of MZMs are their nonlocal correlations. To advance the pursuit of MZMs, new theoretical proposals and new signatures which can reflect the nonlocal correlations of MZMs are hence highly demanded. For example, shot noise and Fano factor in Majorana setups can carry interesting information to identify MZMs [7, 15, 16, 32–38].

Here we propose a T-shaped hybrid structure to detect the MZMs, as illustrated in Fig. 1. The central quantum

dot (QD) acts as a transfer station of electrons and holes. Hence tuning the energy level of the QD is equivalent to tuning the transmission coefficients. The key to probe MZMs is the Majorana-induced crossed Andreev reflection [18, 32, 39, 40]. The ZBCP arises from the crossed Andreev reflection in this T-shaped structure is strongly protected by the energy gap of the superconducting lead because quasiparticle excitations are exponentially suppressed $\sim \exp(\Delta/T)$. Such kind of multiterminal structures with a QD shows excellent maneuverability in the studies of spin-dependent transport in strong Coulomb-correlated systems [41–47].

At zero temperature, we find that the ZBCP of the normal-metal lead is quantized to $2e^2/h$ before braiding, which can be completely induced by the crossed Andreev reflection. This quantized ZBCP is found to be considerably robust against the temperature when the QD is on resonance ($\epsilon_d = 0$). We show that the crossed Andreev reflection dominates over the conventional Andreev reflection when $\epsilon_d \gg \Delta$. Importantly, we find that the Majorana braiding shifts the ZBCPs and arouses a novel kind of crossed Andreev reflection equivalent to the splitting of $3e$ charge quanta, as shown in Fig. 2. Because of the high controllability of QD and the robustness of the predicted signatures, our findings suggest a promising new way to identify MZMs.

This paper is organized as follows. In Sec. II, we introduce the T-shaped hybrid model and explicitly write down their Hamiltonians. In Sec. III, we discuss the electronic transport of the system and provide the corresponding current and conductance formulas, including the analytical expressions for the ZBCPs. In Sec. IV, we present the formula for the shot noise and the Fano factor in terms of appropriate Green's functions. The detailed derivations of the self-energy and the shot noise are given in Appendix A and B.

* zhh98@mail.sysu.edu.cn

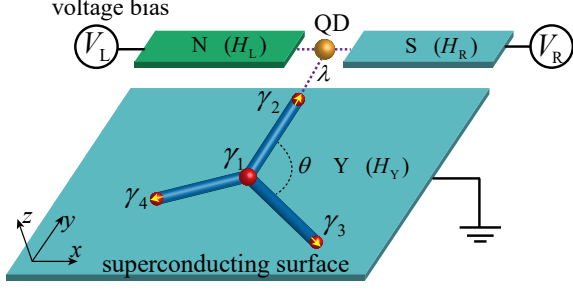


Figure 1: Setup of the T-shaped QD-(N, S, Y) model with the normal-metal lead (N), the superconducting lead (S) and the Majorana Y-junction lead (Y). Following Refs. [48, 49], the Majorana braiding can be implemented on the Y junction by tuning the couplings between the MZMs.

II. MODEL AND FORMULATION

We introduce the three-terminal setup shown in Fig. 1. The three leads are coupled with a central QD and the superconducting lead ensures that the occurrence of crossed Andreev reflection, which protects the ZBCP from quasi-particle excitations. The tunnel-coupled structure can be described by an effective low-energy Hamiltonian:

$$H = H_L + H_R + H_{QD} + H_Y + H_T + H_{T,Y}. \quad (1)$$

The first term in Eq. (1) is the Hamiltonian of the normal-metal lead (N) in Fig. 1, which is characterized by

$$H_L = \sum_{k\sigma} \epsilon_{L,k\sigma} a_{L,k\sigma}^\dagger a_{L,k\sigma}, \quad (2)$$

where $a_{L,k\sigma}^\dagger$ ($a_{L,k\sigma}$) are creation (annihilation) operators with wave vector k and spin $\sigma = \uparrow, \downarrow$, and $\epsilon_{L,k\sigma}$ is the corresponding electron energy. The second term, the Hamiltonian of the superconducting lead (S) in Fig. 1, is given by the BCS theory

$$H_R = \sum_{k\sigma} \epsilon_{R,k\sigma} a_{R,k\sigma}^\dagger a_{R,k\sigma} + \sum_k (\Delta a_{R,k\uparrow}^\dagger a_{R,-k\downarrow}^\dagger + \text{H.c.}). \quad (3)$$

The superconducting energy gap Δ is real here since a unitary transformation has been performed on this Hamiltonian [45, 50]. In this work, we set the applied voltage of the superconducting lead $V_R = 0$. For simplicity, we use the noninteracting Hamiltonian of the QD

$$H_{QD} = \sum_{\sigma} \epsilon_d d_{\sigma}^\dagger d_{\sigma}, \quad (4)$$

where the QD level $\epsilon_d = \epsilon_0 - eV_g/2$ is controlled by the gate voltage V_g . The Hamiltonian of the Majorana Y junction (Y) in Fig. 1 reads

$$H_Y = i \sum_{k=2}^4 t_{1k} \gamma_1 \gamma_k, \quad (5)$$

where the Coulomb coupling constants are $t_{12} = t_{13} = t_{\min}$ and $t_{14} = t_{\max}$ with $t_{\min} \ll t_{\max}$ [48]. Using two fermionic operators $c_1 = (\gamma_1 - i\gamma_4)/2$ and $c_2 = (\gamma_2 - i\gamma_3)/2$, the Hamiltonian H_Y can be represented in the four-dimensional Nambu-spinor space spanned by $c_Y^\dagger = (c_1^\dagger, c_1, c_2^\dagger, c_2)$.

The tunneling Hamiltonian is

$$H_T = H_{T,L} + H_{T,R} = \sum_{k\sigma} v_{L,k} a_{L,k\sigma}^\dagger d_{\sigma} + v_{R,k} a_{R,k\sigma}^\dagger d_{\sigma} + \text{H.c.}, \quad (6)$$

where $v_{L,k}$ and $v_{R,k}$ denote the complex tunneling amplitudes of the normal-metal and superconducting leads, respectively. The coupling between the QD and the Majorana lead is spin-conserving, *i.e.*, the MZM is always tunnel-coupled to electrons in the QD with the same spin orientation [51]. Since we have set the spin orientation of the Rashba spin-orbit coupling along the z -direction in Fig. 1, the spin of each MZM (except γ_1) is parallel to the axial direction of the corresponding nanowire [2, 52]. Defining that the spin- \uparrow direction is along the y -direction, the coupling between the QD and the Majorana lead is given by

$$H_{T,Y} = \lambda d_{\uparrow}^\dagger \gamma_2 + \text{H.c.}, \quad (7)$$

where λ is the coupling amplitude. For simplicity, we assume λ is real.

III. CURRENT AND CONDUCTANCE

The ZBCP arises from the crossed Andreev reflection in this T-shaped structure is a remarkable signature of MZMs. In this section, we first calculate the time-average current by using the nonequilibrium Green's function method [15, 50, 53–56], and then derive the analytic expression of the ZBCP of each lead.

The time-average current of the normal-metal lead is given by

$$\begin{aligned} I_L &= -e \langle \dot{N}_L(t) \rangle \\ &= \frac{e}{h} \int d\omega \text{Re Tr} \{ [G_{QD}^R(\omega) \Sigma_L^<(\omega) + G_{QD}^<(\omega) \Sigma_L^A(\omega)] \tilde{\sigma}_z \}, \end{aligned} \quad (8)$$

where $N_L(t) = \sum_{k\sigma} a_{L,k\sigma}^\dagger(t) a_{L,k\sigma}(t)$ is the total number operator of the electrons in the normal-metal lead. The 4×4 Green's functions $G_{QD}^<(t, t') \equiv -i \langle d(t') d^\dagger(t) \rangle$ and $G_{QD}^R(t, t') \equiv -i \theta(t - t') \langle \{d(t), d^\dagger(t')\} \rangle$ is defined with the Nambu spinors $d^\dagger = (d_\uparrow^\dagger, d_\downarrow, d_\downarrow^\dagger, d_\uparrow)$.

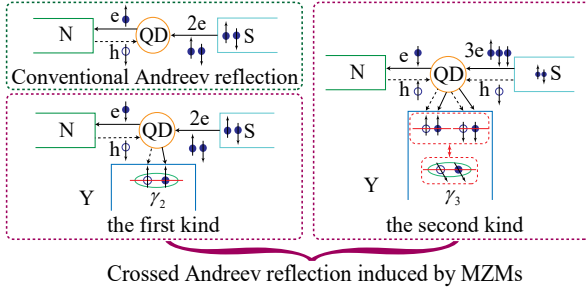


Figure 2: When the Majorana lead is disconnected to the QD ($\lambda = 0$), electrons in the S lead are transferred to the N lead through conventional Andreev reflection; when the Majorana lead is connected to the QD ($\lambda \neq 0$), the MZM γ_2 is the coherent superposition of electrons and holes with only spin \uparrow , which leads to the first kind of crossed Andreev reflection. After braiding, the MZM γ_3 is coupled to the QD. Since γ_3 is the coherent superposition of electrons and holes with spins \uparrow and \downarrow , the second kind of crossed Andreev reflection occurs, which is equivalent to the splitting of charge quanta $3e$. We stress that both kinds of crossed Andreev reflection exist simultaneously after braiding.

The retarded self-energy $\Sigma_L^R(\omega) = [\Sigma_L^A(\omega)]^\dagger = \sum_k \mathcal{H}_{T,L}^\dagger g_L^R(\omega) \mathcal{H}_{T,L}$ is defined with the Nambu spinors $a_{L(R)}^\dagger = (a_{L(R),k\uparrow}^\dagger, a_{L(R),-k\downarrow}^\dagger, a_{L(R),-k\downarrow}^\dagger, a_{L(R),k\uparrow}^\dagger)$. Here $g_L^R(\omega) = (\omega - \mathcal{H}_L + i0^+)^{-1}$ is the corresponding unperturbed Keldysh contour Green's functions of the normal-metal lead. The lesser self-energy is $\Sigma_L^<(\omega) = F_L(\Sigma_L^A(\omega) - \Sigma_L^R(\omega))$, where $F_L = \text{diag}(f_L, f_L, f_L, f_L)$ is the Fermi distribution function matrix with $f_L = f(\omega - eV_L)$ and $\bar{f}_L = f(\omega + eV_L)$. The matrix $\tilde{\sigma}_z = \text{diag}(1, -1, 1, -1)$ describes the different charge of electrons and holes.

The time-average current Eq. (8) is in terms of $\Sigma_L^{R,A,<}(\omega)$ and $G_{QD}^{R,A,<}(\omega)$. This expression can be generalized to I_η by replacing the self-energies $\Sigma_L^{R,A,<}(\omega)$ with $\Sigma_\eta^{R,A,<}(\omega)$ for $\eta = L, R$ and Y representing the normal-metal lead, the superconducting lead and the Majorana lead, respectively. To calculate $\Sigma_\eta^{R,A,<}(\omega)$ concretely, we rewrite the Hamiltonian in Eqs. (2)-(7) with the generalized Nambu representation, which are given by

$$\mathcal{H}_L = \begin{pmatrix} \epsilon_{L,k\uparrow} & 0 & 0 & 0 \\ 0 & -\epsilon_{L,k\downarrow} & 0 & 0 \\ 0 & 0 & \epsilon_{L,k\downarrow} & 0 \\ 0 & 0 & 0 & -\epsilon_{L,k\uparrow} \end{pmatrix}, \quad (9a)$$

$$\mathcal{H}_R = \begin{pmatrix} \epsilon_{R,k\uparrow} & \Delta & 0 & 0 \\ \Delta & -\epsilon_{R,k\downarrow} & 0 & 0 \\ 0 & 0 & \epsilon_{R,k\downarrow} & \Delta \\ 0 & 0 & \Delta & -\epsilon_{R,k\uparrow} \end{pmatrix}, \quad (9b)$$

$$\mathcal{H}_{QD} = \begin{pmatrix} \epsilon_d & 0 & 0 & 0 \\ 0 & -\epsilon_d & 0 & 0 \\ 0 & 0 & \epsilon_d & 0 \\ 0 & 0 & 0 & -\epsilon_d \end{pmatrix}, \quad (9c)$$

$$\mathcal{H}_Y = \begin{pmatrix} -2t_{14} & 0 & it_{12} - t_{13} & it_{12} + t_{13} \\ 0 & 2t_{14} & it_{12} - t_{13} & it_{12} + t_{13} \\ -it_{12} - t_{13} & -it_{12} - t_{13} & 0 & 0 \\ -it_{12} + t_{13} & -it_{12} + t_{13} & 0 & 0 \end{pmatrix}, \quad (9d)$$

$$\mathcal{H}_{T,L(R)} = \begin{pmatrix} v_{L(R),k} & 0 & 0 & 0 \\ 0 & -v_{L(R),k}^* & 0 & 0 \\ 0 & 0 & v_{L(R),k} & 0 \\ 0 & 0 & 0 & -v_{L(R),k}^* \end{pmatrix}, \quad (9e)$$

$$\mathcal{H}_{T,Y} = \begin{pmatrix} 0 & 0 & 0 & 0 \\ 0 & 0 & 0 & 0 \\ \lambda & 0 & 0 & -\lambda \\ \lambda & 0 & 0 & -\lambda \end{pmatrix}. \quad (9f)$$

Assuming that the electron energies in Eqs. 2 and 3 are independent of spins with $\epsilon_{L(R),k\uparrow} = \epsilon_{L(R),k\downarrow} = \epsilon_{L(R),k}$, the retarded self-energies from the couplings between the three leads and the QD are given by

$$\Sigma_L^R(\omega) = -\frac{i}{2} \Gamma_L \begin{pmatrix} 1 & 0 & 0 & 0 \\ 0 & 1 & 0 & 0 \\ 0 & 0 & 1 & 0 \\ 0 & 0 & 0 & 1 \end{pmatrix}, \quad (10)$$

$$\Sigma_R^R(\omega) = -\frac{i}{2} \Gamma_R \beta(\omega) \begin{pmatrix} 1 & -\frac{\Delta}{\omega} & 0 & 0 \\ -\frac{\Delta}{\omega} & 1 & 0 & 0 \\ 0 & 0 & 1 & \frac{\Delta}{\omega} \\ 0 & 0 & \frac{\Delta}{\omega} & 1 \end{pmatrix}, \quad (11)$$

$$\Sigma_Y^R(\omega) = \kappa \Lambda = \kappa \begin{pmatrix} 1 & 0 & 0 & -1 \\ 0 & 0 & 0 & 0 \\ 0 & 0 & 0 & 0 \\ -1 & 0 & 0 & 1 \end{pmatrix}, \quad (12)$$

where $\Gamma_{L(R)} = 2\pi |\nu_{L(R),k}|^2 \rho_{L(R)}$ is the line-width function with $\rho_{L(R)}$ being the density of states. In the wide-band limit, $\Gamma_{L(R)}$ is a constant independent of the frequency ω . Here $\beta(\omega) = \frac{|\omega| \Theta(|\omega| - \Delta)}{\sqrt{\omega^2 - \Delta^2}} + \frac{\omega \Theta(\Delta - |\omega|)}{i\sqrt{\Delta^2 - \omega^2}}$ is the dimensionless BCS density of states. Neglecting the contribution of t_{\min} , we have $\kappa \approx \frac{-8\lambda^2 t_{\max}^2 + 2\lambda^2 (\omega^+)^2}{-4t_{\max}^2 \omega^+ + (\omega^+)^3}$ with $\omega^+ = \omega + i0^+$.

The lesser Green's function of the QD can be obtained via the Keldysh equation $G_{QD}^<(\omega) = G_{QD}^R(\omega) \Sigma_{TOT}^<(\omega) G_{QD}^A(\omega)$, with $\Sigma_{TOT}^< = \sum_\eta \Sigma_\eta^<$. In the calculation of the time-average current, we can take $\Sigma_Y^< = 0$ (see Appendix A for details). In the case of $|eV_L| < |\Delta|$, analytical calculations for the time-average

current yield $I_\eta = \frac{e}{2h} \int d\omega (f_L - \bar{f}_L) T_\eta(\omega)$, which means that only Andreev reflection processes contribute to the electronic transport of the system. Since the system is in a stationary regime, the total current is conserved, *i.e.*, $\sum_\eta I_\eta = 0$.

The differential conductances of the leads η at zero temperature are obtained by $G_\eta = \frac{dI_\eta}{dV_L}$. Especially, the ZBCPs at zero temperature are

$$\lim_{eV_L \rightarrow 0} G_L(eV_L) = \begin{cases} \frac{2e^2}{h}, & \lambda \neq 0, \\ \frac{e^2}{h} \frac{16\Gamma_L^2 \Gamma_R^2}{(\Gamma_L^2 + \Gamma_R^2 + 4\epsilon_d^2)^2}, & \lambda = 0, \end{cases} \quad (13)$$

$$\lim_{eV_L \rightarrow 0} G_R(eV_L) = \begin{cases} -\frac{e^2}{h} \frac{4\Gamma_R^2}{\Gamma_L^2 + \Gamma_R^2 + 4\epsilon_d^2}, & \lambda \neq 0, \\ -\frac{e^2}{h} \frac{16\Gamma_L^2 \Gamma_R^2}{(\Gamma_L^2 + \Gamma_R^2 + 4\epsilon_d^2)^2}, & \lambda = 0, \end{cases} \quad (14)$$

$$\lim_{eV_L \rightarrow 0} G_Y(eV_L) = \begin{cases} -\frac{e^2}{h} \frac{2(\Gamma_L^2 - \Gamma_R^2 + 4\epsilon_d^2)}{\Gamma_L^2 + \Gamma_R^2 + 4\epsilon_d^2}, & \lambda \neq 0, \\ 0, & \lambda = 0. \end{cases} \quad (15)$$

When $\lambda = 0$, the Majorana Y junction is disconnected with the QD, and the remaining part is reduced to an N-QD-S structure. The maximal ZBCP in Eq. (13) is equal to $4e^2/h$ when the QD is symmetrically coupled ($\Gamma_L = \Gamma_R$) and on resonance ($\epsilon_d = 0$), in accord with the previous results of Ref. [43]. When $\lambda \neq 0$, the ZBCP of the normal-metal lead in this three-terminal structure equals a quantized value $2e^2/h$, consistent with the famous conductance peak for the N-TS tunneling. As depicted in Fig. 3, the ZBCP is obviously broad for $\epsilon_d = 0$ and becomes sharp for large ϵ_d . The QD acts as a transfer station of electrons and holes, which means that the energy level of the QD is the tunnel barrier of the system. Hence the broadening of the ZBCP arises from the junction transparency effect and the height of the ZBCP is not affected. This quantized ZBCP is caused by the perfect Majorana-induced Andreev reflection. In the next section, we will show that the local Andreev reflection can be completely suppressed by increasing ϵ_d , and only the crossed Andreev reflection remains. We emphasize again that this ZBCP of $2e^2/h$ can completely arise from the crossed Andreev reflection, which is strongly protected by the superconducting gap Δ [21]. Moreover, the results of Eqs. 14 and 15 show that the ZBCPs of both the superconducting and the Majorana leads are insensitive to the nonzero coupling amplitude λ , but only dependent on Γ_L , Γ_R and ϵ_d .

The discussion can easily extend to finite temperature regimes. As shown in Fig. 4, the ZBCP of the normal-metal lead is no longer quantized to $2e^2/h$, since the Fermi distribution is smoothly dependent on the temperature T , which is called the thermal broadening. Nevertheless, we find that the effect of the thermal broadening is significantly suppressed by large junction transparency ($\epsilon_d = 0$). In Fig. 4, the ZBCP is pretty close to $2e^2/h$ when $k_B T < \Delta/20$. Such a temperature condition can be met in the experiment, *e.g.*, see Ref. [27], in which the induced superconducting gap of the InSb

nanowires is $\Delta \approx 250\mu\text{eV}$ and the minimized temperature is $k_B T \approx 4.3\mu\text{eV}$.

IV. SHOT NOISE AND FANO FACTOR

In addition to the time-average current, the shot noise can reveal the fluctuation of the current and provides useful information about MZMs [7, 32, 35, 57]. The shot noise, defined as the correlation function of the current fluctuations between leads η and η' , takes the form $S_{\eta\eta'}(t, t') = \langle \{\delta I_\eta(t), \delta I_{\eta'}(t')\} \rangle$, where $\delta I_\eta(t) = \hat{I}_\eta(t) - I_\eta$, and $\hat{I}_\eta(t) = -e\dot{N}_\eta(t)$. The time-average current I_η has been obtained by Eq. (8). With the use of the Wick's theorem and the S-matrix expansion [15, 47], we can reduce the expression of the shot noise in terms of Green's functions. After Fourier transform, we obtain the expression of shot noise in the frequency space $S_{\eta\eta'}(\omega')$. The calculation of the shot noise is shown explicitly in Appendix B.

Following Ref. [58], in multi-terminal systems, the shot noise $S_{\eta\eta'}(\omega')$ with $\eta = \eta'$ must be positive; conversely, that with $\eta \neq \eta'$ must be negative. This property can be verified by the numerical calculation of $S_{\eta\eta}(0)$ in the following. The zero-frequency Fano factor, defined by the ratio $F_\eta = S_{\eta\eta}(0)/2eI_\eta$, can gain insight into the nature of charge quanta transferred to lead η [35, 59, 60].

The discussion will focus on the case of small transparency ($\epsilon_d \gg \Delta$) since we find that the Fano factors are quantized in this regime. In Fig. 5, we present the Fano factors at zero temperature as functions of ϵ_d/Δ for a specific realization. In the case of $\lambda = 0$, the remaining N-QD-S junction shows a doubled shot noise in Fano factors $F_L(\epsilon_d \gg \Delta) = -F_R(\epsilon_d \gg \Delta) = 2$ due to the transport of Cooper pairs through conventional Andreev reflection [61]. When the Majorana Y junction is connected to the QD with $\lambda \neq 0$, we find $F_L(\epsilon_d \gg \Delta) = -F_Y(\epsilon_d \gg \Delta) = 1$ and $|F_R(\epsilon_d \gg \Delta)| = 2$. The results denote that the unit of charge transferred between the QD and the normal-metal lead is e as well as the Majorana lead, while the unit of charge transferred between the QD and the superconducting lead is $2e$. This is the process of the first kind of crossed Andreev reflection. A hole from the left lead is reflected as an electron into the Majorana lead, while a Cooper pair from the superconducting lead is reflected as a hole into the Majorana lead and an electron into the normal-metal lead [32], as shown in Fig. 2. The holes transferred through crossed Andreev reflection act as facilitators to propel the splitting of Cooper pairs, and do not contribute to the transferred charge. In this regime, local Andreev reflection is fully suppressed, and the first kind of crossed Andreev reflection dominates.

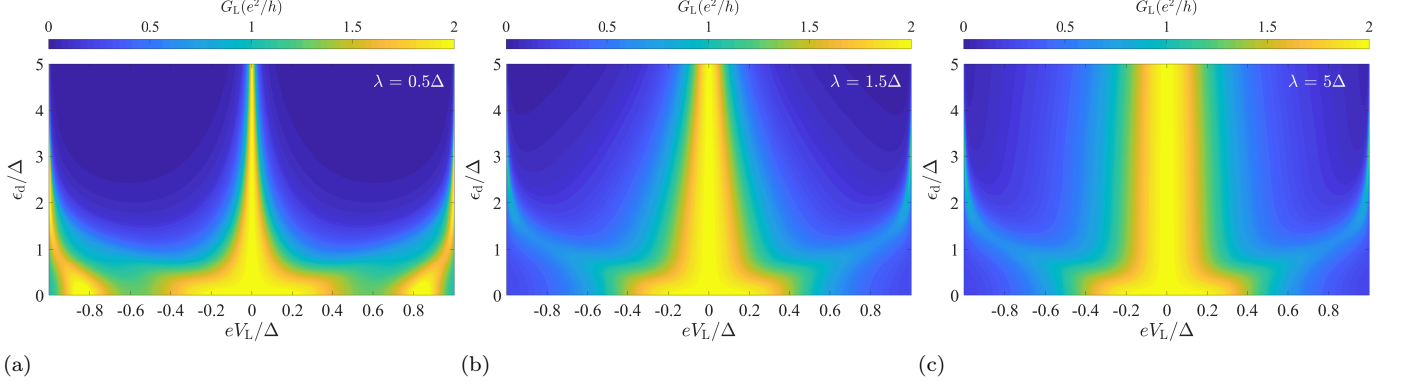


Figure 3: Differential conductance spectra of the normal-metal lead as functions of eV_L/Δ and ϵ_d/Δ at zero temperature. The parameters are $\Gamma_L = \Gamma_R = 0.8\Delta$, $t_{\min} = 0.001\Delta$, and $t_{\max} = \Delta$.

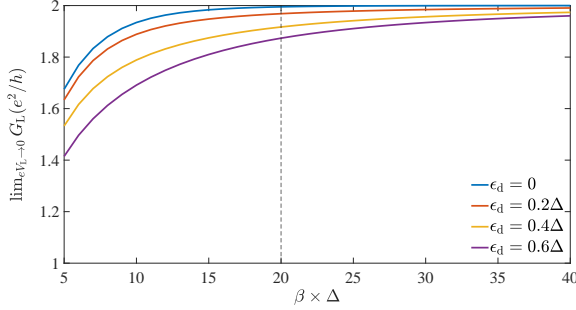


Figure 4: ZBCP of the normal-metal lead as a function of finite temperature. The parameters are $\Gamma_L = \Gamma_R = 0.8\Delta$, $\lambda = \Delta$, $t_{\min} = 10^{-3}\Delta$, and $t_{\max} = \Delta$.

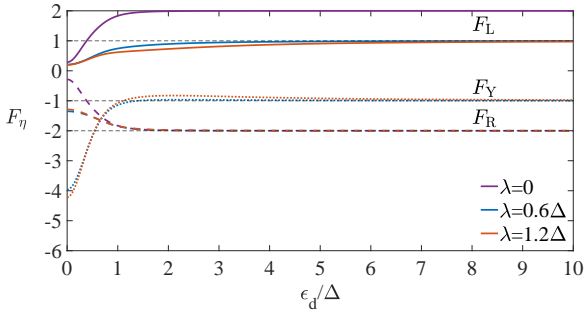


Figure 5: Fano factors at zero temperature of the left lead (solid lines), right lead (dashed lines) and Majorana lead (dotted lines) as functions of ϵ_d . The parameters are $eV_L = 0.5\Delta$, $\Gamma_L = \Gamma_R = 0.8\Delta$, $t_{\min} = 0.001\Delta$, and $t_{\max} = \Delta$.

V. SIGNATURES OF THE MAJORANA BRAIDING

Now we braid the MZMs by taking $\gamma_2 \rightarrow -\gamma_3$ and $\gamma_3 \rightarrow \gamma_2$. The QD is connected to the Majorana Y junction

through γ_3 . Using the Nambu spinors and Eq. (5), we can easily obtain the Hamiltonian of the Majorana Y junction $\tilde{\mathcal{H}}_Y$ after braiding. Given that the angle of spin orientations between γ_2 and γ_3 is θ , the spin-conserving coupling is then given by $\tilde{H}_{T,Y} = -i\lambda\gamma_3\tilde{d}_\uparrow + \text{H.c.}$, where \tilde{d}_\uparrow (\tilde{d}_\downarrow) is the electron operators of the QD with the same (opposite) spin orientation described by γ_3 with

$$\begin{pmatrix} \tilde{d}_\uparrow \\ \tilde{d}_\downarrow \end{pmatrix} = \begin{pmatrix} \cos \frac{\theta}{2} & \sin \frac{\theta}{2} \\ -\sin \frac{\theta}{2} & \cos \frac{\theta}{2} \end{pmatrix} \begin{pmatrix} d_\uparrow \\ d_\downarrow \end{pmatrix}. \quad (16)$$

For the Majorana Y junction sketched in Fig. 1, the spin orientation angle is $\theta = \frac{2}{3}\pi$. Such a braiding process is equivalent to involving spin-flip tunneling between the QD and Majorana lead. After braiding, we can obtain the ZBCPs by

$$\lim_{eV_L \rightarrow 0} \tilde{G}_L(eV_L) = \begin{cases} \frac{e^2}{h} \frac{8\Gamma_L^2((\Gamma_L^2 + \Gamma_R^2 + 4\epsilon_d^2)^2 + \Gamma_R^4 + \Gamma_L^2\Gamma_R^2)}{(4\Gamma_L^2 + \Gamma_R^2)(\Gamma_L^2 + \Gamma_R^2 + 4\epsilon_d^2)^2}, & \lambda \neq 0, \\ \frac{e^2}{h} \frac{16\Gamma_L^2\Gamma_R^2}{(\Gamma_L^2 + \Gamma_R^2 + \epsilon_d^2)^2}, & \lambda = 0, \end{cases} \quad (17)$$

$$\lim_{eV_L \rightarrow 0} \tilde{G}_R(eV_L) = \begin{cases} -\frac{e^2}{h} \frac{4\Gamma_L^2\Gamma_R^2(5\Gamma_L^2 + 5\Gamma_R^2 + 12\epsilon_d^2)}{(4\Gamma_L^2 + \Gamma_R^2)(\Gamma_L^2 + \Gamma_R^2 + 4\epsilon_d^2)^2}, & \lambda \neq 0, \\ -\frac{e^2}{h} \frac{16\Gamma_L^2\Gamma_R^2}{(\Gamma_L^2 + \Gamma_R^2 + \epsilon_d^2)^2}, & \lambda = 0, \end{cases} \quad (18)$$

$$\lim_{eV_L \rightarrow 0} \tilde{G}_Y(eV_L) = \begin{cases} -\frac{e^2}{h} \frac{4\Gamma_L^2(2\Gamma_L^2 - \Gamma_R^2 + 8\epsilon_d^2)}{(4\Gamma_L^2 + \Gamma_R^2)(\Gamma_L^2 + \Gamma_R^2 + 4\epsilon_d^2)}, & \lambda \neq 0, \\ 0, & \lambda = 0. \end{cases} \quad (19)$$

When $\lambda = 0$, the result is the same as that before braiding; when $\lambda \neq 0$, the occurrence of spin-flip tunneling shifts the ZBCP. We plot the differential conductance of the normal-metal lead after the Majorana braiding in Fig. 6 for comparison to Fig. 3. Particularly, if the QD is symmetrically coupled ($\Gamma_L = \Gamma_R = \Gamma$), the ZBCP of the normal-metal lead maximally shifts to $2.4e^2/h$ for $\epsilon_d = 0$ and $1.6e^2/h$ for $\epsilon_d \gg \Delta$, which can act a robust

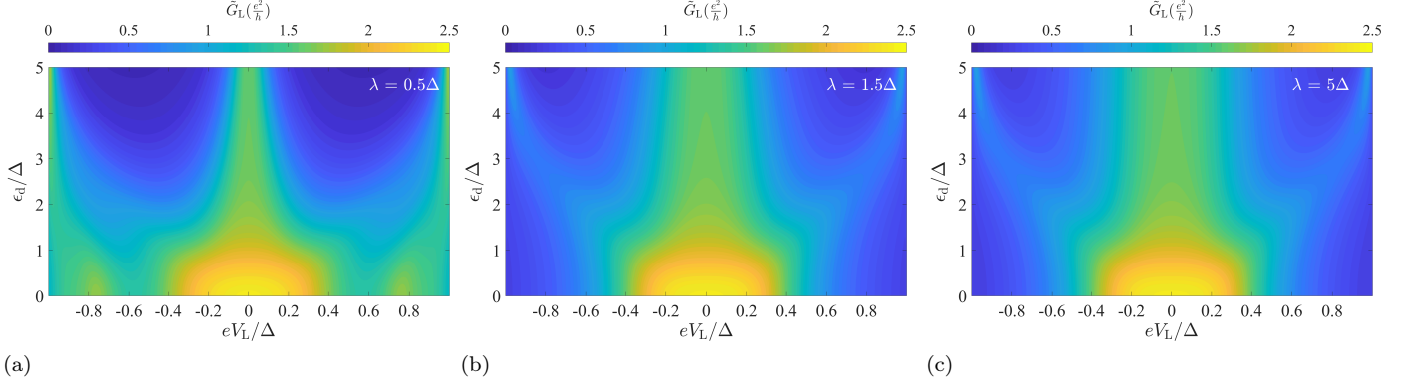


Figure 6: Differential conductance spectra of the normal-metal lead as a function of eV_L/Δ and ϵ_d/Δ after braiding at zero temperature. The parameters are the same in Fig. 3

hint of Majorana braiding. With the increasing of ϵ_d , the ZBCP gets broadened and its height gets lower concurrently. As shown in Fig. 7., the thermal broadening effect can also be suppressed by taking $\epsilon_d = 0$ and each solid line is closed to the corresponding zero-temperature limit when $k_B T < \Delta/20$. Consequently, it is appropriate for the observation of the ZBCP with a large junction transparency.

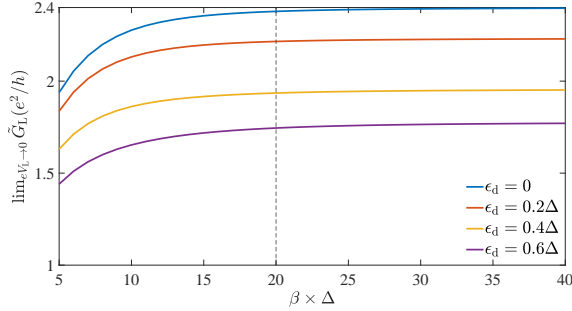


Figure 7: ZBCP of the normal-metal lead after braiding as a function of the finite temperature. The parameters are the same as in Fig. 4.

The Fano factors after braiding are also quantized, but $2 < |\tilde{F}_R(\epsilon_d \gg \Delta)| < 3$, *i.e.*, the unit of charge transferred between the QD and the superconducting lead is larger than that of a Cooper pair, as shown Fig. 8. This result is induced by involving both spins \uparrow and \downarrow in the coupling between the QD and the MZM γ_3 . As illustrated in Fig. 2, the second kind of crossed Andreev reflection occurs after the Majorana braiding.

Specifically, a Cooper pair transferred between the QD and the superconducting lead is accompanied by an extra electron and a hole, which leads to the $3e$ charge quanta. One electron of the $3e$ charge quanta is reflected as an electron into the normal-metal lead, while the other two are reflected as holes into the Majorana lead. Such a process of charge transmission is equivalent to the splitting

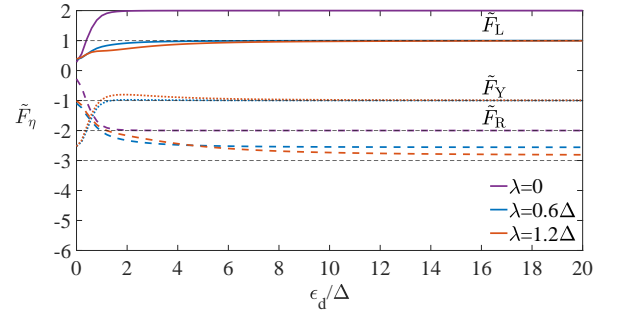


Figure 8: Fano factors after braiding at zero temperature of the left lead (solid lines), right lead (dashed lines) and Majorana lead (dotted lines) as functions of ϵ_d . The parameters are the same as in Fig. 5.

of the $3e$ charge quanta.

Given that the electrons coupled to the MZM γ_3 are composed of spin- \uparrow and \downarrow electrons with a certain weight depending on the angle θ (see Eq. (16)), both kinds of crossed Andreev reflection exist simultaneously, which leads to $2 < |\tilde{F}_R(\epsilon_d \gg \Delta)| < 3$. As shown in Fig. 8, the second kind of crossed Andreev reflection gains the dominance of the tunneling processes (corresponding to $|\tilde{F}_R(\epsilon_d \gg \Delta)| \rightarrow 3$) with increasing λ . As for the Majorana lead, the acceptance of spin- \uparrow and \downarrow electrons with a certain weight is equivalent to the acceptance of an electron with spin polarization angle θ in each current pulse, which gives rise to $|\tilde{F}_Y(\epsilon_d \gg \Delta)| = 1$. The units of the charge transferred between the normal-metal lead and the QD for both kinds of crossed Andreev reflection are identical, so the Fano factor of the normal-metal lead stays at $|\tilde{F}_L(\epsilon_d \gg \Delta)| = 1$, the same as that before braiding.

VI. CONCLUSION

We have studied the ZBCPs and the Fano factors of the T-shaped structure. We have shown that the ZBCP of the normal-metal lead is always quantized to $2e^2/h$ at zero temperature before braiding, which is quite robust at finite temperature when the QD is on-resonance. This quantized conductance can entirely arise from the Majorana-induced crossed Andreev reflection, which is protected by the energy gap of the superconducting lead. After Majorana braiding, the quantized ZBCP shifts and becomes dependent on the line widths Γ_L , Γ_R and the QD level ϵ_d . This variation is owing to the introduction of spin-flip tunneling between the Majorana lead and the QD after braiding. By analyzing the quantized Fano factors, we have found that the crossed Andreev reflection dominates over the conventional Andreev reflection when $\epsilon_d \gg \Delta$. We have also found a novel kind of crossed Andreev reflection equivalent to the splitting of the $3e$ charge quanta. The quantized ZBCPs and Fano factors induced by the nonlocal crossed Andreev reflection provide strong fingerprint for MZMs.

ACKNOWLEDGMENTS

We would like to thank Ze-Min Huang and Zhongbo Yan for helpful discussions. This work is supported in part by the National Natural Science Foundation of China under Grants No. 11875327, the Fundamental Research Funds for the Central Universities, and the Sun Yat-Sen University Science Foundation.

Appendix A: CALCULATION OF $\Sigma_Y^<$

In this section, we present the details of the analytical calculation of the terms containing $\Sigma_Y^<$ in Eqs. 8. The less self-energy from the Majorana lead is given by

$$\Sigma_Y^< = F_Y(\Sigma_Y^A - \Sigma_Y^R) = -i2F_Y \text{Im}\Sigma_Y^R, \quad (\text{A1})$$

where

$$Q_1(\omega) = i\pi \frac{-8\lambda^2 t_{\max}^2}{4t_{\max}^2 - 3\omega^2} \left| \frac{(4t_{\max}^2 - 3\omega^2)^2}{-(4t_{\max}^2 - 3\omega^2)^2 - 6\omega^2(4t_{\max}^2 - \omega^2)} \right|, \quad (\text{A11})$$

$$Q_2(\omega) = -i\pi \frac{2\lambda^2 \omega^2}{4t_{\max}^2 + \omega^2} \left| \frac{(4t_{\max}^2 + \omega^2)^2}{(-4t_{\max}^2 + 3\omega^2)(4t_{\max}^2 + \omega^2) - 2\omega^2(-4t_{\max}^2 + \omega^2)} \right|. \quad (\text{A12})$$

It is obvious that $Q_1(0) = -2i\pi\lambda^2$, $Q_1(\pm 2t_{\max}) = i\pi\lambda^2$, $Q_2(0) = 0$ and $Q_2(\pm 2t_{\max}) = -i\pi\lambda^2$. Since the electron-hole symmetric gives $G_{\text{QD}}^R(-\omega) = -[G_{\text{QD}}^R(\omega)]^*$, i.e., $G_{\text{QD}}^R(0)$ is a pure virtual function. Note that

where Σ_Y^R is determined by

$$\kappa \approx \frac{-8\lambda^2 t_{\max}^2}{-4t_{\max}^2 \omega^+ + (\omega^+)^3} + \frac{2\lambda^2 (\omega^+)^2}{-4t_{\max}^2 \omega^+ + (\omega^+)^3}, \quad (\text{A2})$$

with $\omega^+ = \omega + i0^+$, as we mentioned in the main text (see Eq. (12)). We use the notation κ_1 and κ_2 to denote the first term and the second term of κ , respectively. Neglecting the high-order terms of $(i0^+)^{n \geq 2}$, we can obtain the following expressions:

$$\kappa_1 = \frac{-8\lambda^2 t_{\max}^2}{(-4t_{\max}^2 \omega + \omega^3) - (4t_{\max}^2 - 3\omega^2)(i0^+)}, \quad (\text{A3})$$

$$\kappa_2 = \frac{2\lambda^2 \omega^2}{\omega(-4t_{\max}^2 + \omega^2) + (4t_{\max}^2 + \omega^2)(i0^+)}. \quad (\text{A4})$$

Using the limitation

$$\lim_{\eta \rightarrow 0^+} \frac{1}{x \pm i\eta} = \mathcal{P} \frac{1}{x} \mp i\pi \delta(x), \quad (\text{A5})$$

we can obtain

$$i\text{Im}(\kappa_1) = i\pi \frac{-8\lambda^2 t_{\max}^2}{4t_{\max}^2 - 3\omega^2} \delta\left(\frac{-4t_{\max}^2 \omega + \omega^3}{4t_{\max}^2 - 3\omega^2}\right), \quad (\text{A6})$$

$$i\text{Im}(\kappa_2) = -i\pi \frac{2\lambda^2 \omega^2}{4t_{\max}^2 + \omega^2} \delta\left(\frac{-4t_{\max}^2 \omega + \omega^3}{4t_{\max}^2 + \omega^2}\right). \quad (\text{A7})$$

Using the relationship

$$\delta(\phi(x)) = \sum_j \frac{1}{|\phi'(x)|} \delta(x - x_j), \quad (\text{A8})$$

with $\phi(x_j) = 0$, the imaginary part of κ_1 and κ_2 reduce to

$$i\text{Im}(\kappa_1) = Q_1(\omega)[\delta(\omega) + \delta(\omega - 2t_{\max}) + \delta(\omega + 2t_{\max})], \quad (\text{A9})$$

$$i\text{Im}(\kappa_2) = Q_2(\omega)[\delta(\omega) + \delta(\omega - 2t_{\max}) + \delta(\omega + 2t_{\max})], \quad (\text{A10})$$

the imaginary part of $G_{\text{QD}}^R(0)$ is tiny, we can obtain $G_{\text{QD}}^R(0) \approx 0$. For example, the terms containing $\Sigma_Y^<$ in Eq. (8) are calculated by

$$\begin{aligned}
\int d\omega G_{\text{QD}}^R(\omega) \Sigma_Y^<(\omega) &\propto \int d\omega G_{\text{QD}}^R(\omega) [i\text{Im}(\kappa_1 + \kappa_2)] \\
&= -2i\pi\lambda^2 G_{\text{QD}}^R(0) \\
&= 0,
\end{aligned} \tag{A13}$$

$$\begin{aligned}
&\int d\omega G_{\text{QD}}^R(\omega) \Sigma_Y^<(\omega) G_{\text{QD}}^A(\omega) \Sigma_\eta^A(\omega) \\
&= i\pi\lambda^2 [G_{\text{QD}}^R(0) \Lambda G_{\text{QD}}^A(0) \Sigma_\eta^A(0)] \\
&= 0.
\end{aligned} \tag{A14}$$

Hence we can take $\Sigma_Y^< = 0$ in the calculation of the time-average current and the shot noise.

Appendix B: CALCULATION OF THE SHOT NOISE $S_{\eta\eta'}(\omega')$

and

In this section, we review the formalism for the shot noise which will be used in the main text [15, 47]. Without loss of generality, the Hamiltonian of a multi-terminal systems with a central QD is

$$H = \sum_{\eta} H_{\eta} + H_{\text{QD}} + H_T, \tag{B1}$$

where $H_{\eta} = \sum_{k\sigma} \epsilon_{\eta,k\sigma} a_{\eta,k\sigma}^{\dagger} a_{\eta,k\sigma}$ and $H_{\text{QD}} = \sum_{\sigma} \epsilon_{\text{d}} d_{\sigma}^{\dagger} d_{\sigma}$.

The tunneling Hamiltonian is given by

$$H_T = \sum_{\eta k\sigma} (t_{k\sigma} a_{\eta,k\sigma}^{\dagger} d_{\sigma} + t_{\sigma}^* d_{\sigma}^{\dagger} a_{\eta,k\sigma}), \tag{B2}$$

where $t_{k\sigma}$ is the tunneling amplitude between the leads η and the QD

The definition of the shot noise is given by

$$\begin{aligned}
S_{\eta\eta'}(t, t') &= \left\langle \{ \delta \hat{I}_{\eta}(t), \delta \hat{I}_{\eta'}(t') \} \right\rangle \\
&= \left\langle \{ \hat{I}_{\eta}(t), \hat{I}_{\eta'}(t') \} \right\rangle - 2 \left\langle \hat{I}_{\eta}(t) \right\rangle \left\langle \hat{I}_{\eta'}(t') \right\rangle \\
&= -\frac{e^2}{\hbar} \sum_{kk'\sigma\sigma'} \left\{ t_{k\sigma} t_{k'\sigma'} \left\langle a_{\eta k\sigma}^{\dagger}(t) d_{\sigma}(t) a_{\eta' k'\sigma'}^{\dagger}(t') d_{\sigma'}(t') \right\rangle \right. \\
&\quad - t_{k\sigma} t_{k'\sigma'}^* \left\langle a_{\eta k\sigma}^{\dagger}(t) d_{\sigma}(t) d_{\sigma'}^{\dagger}(t') a_{\eta' k'\sigma'}(t') \right\rangle \\
&\quad - t_{k\sigma}^* t_{k'\sigma'} \left\langle d_{\sigma}^{\dagger}(t) a_{\eta k\sigma}(t) a_{\eta' k'\sigma'}^{\dagger}(t') d_{\sigma'}(t') \right\rangle \\
&\quad \left. + t_{k\sigma}^* t_{k'\sigma'}^* \left\langle d_{\sigma}^{\dagger}(t) a_{\eta k\sigma}(t) d_{\sigma'}^{\dagger}(t') a_{\eta' k'\sigma'}(t') \right\rangle \right\} + \text{H.C.} - 2 \left\langle \hat{I}_{\eta}(t) \right\rangle \left\langle \hat{I}_{\eta'}(t') \right\rangle.
\end{aligned} \tag{B3}$$

Let's define the two-particle Green's functions,

$$G_1^{(2)}(\tau, \tau') = i^2 \left\langle T_C a_{\eta k \sigma}^\dagger(\tau) d_\sigma(\tau) a_{\eta' k' \sigma'}^\dagger(\tau') d_{\sigma'}(\tau') \right\rangle, \quad (\text{B4})$$

$$G_2^{(2)}(\tau, \tau') = i^2 \left\langle T_C a_{\eta k \sigma}^\dagger(\tau) d_\sigma(\tau) d_{\sigma'}^\dagger(\tau') a_{\eta' k' \sigma'}(\tau') \right\rangle, \quad (\text{B5})$$

$$G_3^{(2)}(\tau, \tau') = i^2 \left\langle T_C d_\sigma^\dagger(\tau) a_{\eta k \sigma}(\tau) a_{\eta' k' \sigma'}^\dagger(\tau') d_{\sigma'}(\tau') \right\rangle, \quad (\text{B6})$$

$$G_4^{(2)}(\tau, \tau') = i^2 \left\langle T_C d_\sigma^\dagger(\tau) a_{\eta k \sigma}(\tau) d_{\sigma'}^\dagger(\tau') a_{\eta' k' \sigma'}(\tau') \right\rangle, \quad (\text{B7})$$

so that the shot noise can be expressed as

$$S_{\eta\eta'}(t, t') = \frac{e^2}{\hbar} \sum_{kk', \sigma\sigma'} \left\{ t_{k\sigma} t_{k'\sigma'} G_1^{(2)>}(t, t') - t_{k\sigma} t_{k'\sigma'}^* G_2^{(2)>}(t, t') \right. \\ \left. - t_{k\sigma}^* t_{k'\sigma'} G_3^{(2)>}(t, t') + t_{k\sigma}^* t_{k'\sigma'}^* G_4^{(2)>}(t, t') \right\} + \text{H.C.} - 2 \left\langle I_\eta(t) \right\rangle \left\langle I_{\eta'}(t') \right\rangle, \quad (\text{B8})$$

where $G_i^{(2)>}(t, t')$ can be obtained from $G_i^{(2)}(\tau, \tau')$ via analytical continuation. The expression of $G_i^{(2)}(\tau, \tau')$ can be reduced by using the S-matrix expansion and Wick's theorem, and more details can be found in Ref. [47]. Here we show the results after simplification,

$$G_1^{(2)}(\tau, \tau') = t_{k\sigma}^* t_{k'\sigma'}^* \int \int d\tau_1 d\tau_2 G_{\eta, k\sigma\sigma}(\tau_1, \tau) G_{\eta', k'\sigma'\sigma'}(\tau_2, \tau') \quad (\text{B9})$$

$$\times [G_{\text{QD}, \sigma\sigma}(\tau, \tau_1) G_{\text{QD}, \sigma'\sigma'}(\tau', \tau_2) - G_{\text{QD}, \sigma\sigma'}(\tau, \tau_2) G_{\text{QD}, \sigma'\sigma}(\tau', \tau_1)], \quad (\text{B10})$$

$$G_2^{(2)}(\tau, \tau') = -\delta_{kk'\sigma'\sigma'\eta\eta'} G_{\eta, k\sigma\sigma}(\tau', \tau) G_{\text{QD}, \sigma\sigma'}(\tau, \tau') \\ + t_{k\sigma}^* t_{k'\sigma'} \int \int d\tau_1 d\tau_2 G_{\eta, k\sigma\sigma}(\tau_1, \tau) G_{\eta', k'\sigma'\sigma'}(\tau', \tau_2) \quad (\text{B11})$$

$$\times [G_{\text{QD}, \sigma\sigma}(\tau, \tau_1) G_{\text{QD}, \sigma'\sigma'}(\tau_2, \tau') - G_{\text{QD}, \sigma\sigma'}(\tau, \tau') G_{\text{QD}, \sigma'\sigma}(\tau_2, \tau_1)], \quad (\text{B12})$$

$$G_3^{(2)}(\tau, \tau') = [G_2^{(2)}(\tau, \tau')]^*, \quad (\text{B13})$$

$$G_4^{(2)}(\tau, \tau') = [G_1^{(2)}(\tau, \tau')]^*, \quad (\text{B14})$$

where $G_{\eta, k\sigma\sigma}(\tau_1, \tau) = -i \left\langle T_C a_{\eta k \sigma}(\tau_1) a_{\eta k \sigma}^\dagger(\tau) \right\rangle$ and $G_{\text{QD}, \sigma\sigma'}(\tau, \tau_2) = -i \left\langle T_C d_\sigma(\tau) d_{\sigma'}^\dagger(\tau_2) \right\rangle$. The two-particle Green's functions above can be decomposed into the connected and disconnected terms, i.e., $G_i^{(2)}(\tau, \tau') = G_{i, \text{disc}}^{(2)}(\tau, \tau') + G_{i, \text{conn}}^{(2)}(\tau, \tau')$. The disconnected terms are given by

$$G_{1, \text{disc}}^{(2)}(\tau, \tau') = t_{k\sigma}^* t_{k'\sigma'}^* \int d\tau_1 G_{\text{QD}, \sigma\sigma}(\tau, \tau_1) G_{\eta, k\sigma\sigma}(\tau_1, \tau^+) \int d\tau_2 G_{\text{QD}, \sigma'\sigma'}(\tau', \tau_2) G_{\eta', k'\sigma'\sigma'}(\tau_2, \tau'^+), \quad (\text{B15})$$

$$G_{2, \text{disc}}^{(2)}(\tau, \tau') = t_{k\sigma}^* t_{k'\sigma'} \int d\tau_1 G_{\text{QD}, \sigma\sigma}(\tau, \tau_1) G_{\eta, k\sigma\sigma}(\tau_1, \tau^+) \int d\tau_2 G_{\eta', k'\sigma'\sigma'}(\tau', \tau_2) G_{\text{QD}, \sigma'\sigma'}(\tau_2, \tau'^+), \quad (\text{B16})$$

$$G_{3, \text{disc}}^{(2)}(\tau, \tau') = [G_{2, \text{disc}}^{(2)}(\tau, \tau')]^*, \quad (\text{B17})$$

$$G_{4, \text{disc}}^{(2)}(\tau, \tau') = [G_{1, \text{disc}}^{(2)}(\tau, \tau')]^*. \quad (\text{B18})$$

The analytic continuation rules give

$$G_{1,\text{disc}}^{(2)>}(t, t') = t_{k\sigma}^* t_{k'\sigma'}^* F_{\eta,k\sigma}(t, t) F_{\eta',k'\sigma'}(t', t'), \quad (\text{B19})$$

$$G_{2,\text{disc}}^{(2)>}(t, t') = -t_{k\sigma}^* t_{k'\sigma'} F_{\eta,k\sigma}(t, t) F_{\eta',k'\sigma'}^*(t', t'), \quad (\text{B20})$$

$$G_{3,\text{disc}}^{(2)>}(t, t') = -t_{k\sigma} t_{k'\sigma'}^* F_{\eta,k\sigma}^*(t, t) F_{\eta',k'\sigma'}(t', t'), \quad (\text{B21})$$

$$G_{4,\text{disc}}^{(2)>}(t, t') = t_{k\sigma} t_{k'\sigma'} F_{\eta,k\sigma}^*(t, t) F_{\eta',k'\sigma'}^*(t', t'), \quad (\text{B22})$$

where

$$F_{\eta,k\sigma}(t, t) = \int d\tau_1 G_{\text{QD},\sigma\sigma}^R(t, t_1) G_{\eta,k\sigma\sigma}^{<}(t_1, t) + G_{\text{QD},\sigma\sigma}^{<}(t, t_1) G_{\eta,k\sigma\sigma}^A(t_1, t). \quad (\text{B23})$$

The total contribution of the disconnected terms is

$$\begin{aligned} \left\langle \left\{ \hat{I}_\eta(t), \hat{I}_{\eta'}(t') \right\} \right\rangle_{\text{disc}} &= \frac{e^2}{\hbar} \sum_{kk'\sigma\sigma'} \left\{ t_{k\sigma} t_{k'\sigma'} G_{1,\text{disc}}^{(2)>}(t, t') - t_{k\sigma} t_{k'\sigma'}^* G_{2,\text{disc}}^{(2)>}(t, t') \right. \\ &\quad \left. - t_{k\sigma}^* t_{k'\sigma'} G_{3,\text{disc}}^{(2)>}(t, t') + t_{k\sigma}^* t_{k'\sigma'}^* G_{4,\text{disc}}^{(2)>}(t, t') \right\} + \text{H.C.} \\ &= 2 \frac{e^2}{\hbar} \sum_{kk'\sigma\sigma'} |t_{k\sigma}|^2 |t_{k'\sigma'}|^2 \left[F_{\eta,k\sigma}(t, t) + F_{\eta,k\sigma}^*(t, t) \right] \left[F_{\eta',k'\sigma'}(t', t') + F_{\eta',k'\sigma'}^*(t', t') \right]. \end{aligned} \quad (\text{B24})$$

Note that $\Sigma_{\eta,k\sigma\sigma}^{<} = |t_{k\sigma}|^2 G_{\eta,k\sigma\sigma}^{<}(t_1, t)$, the time-average current in Eq. (8) can be written as

$$\left\langle \hat{I}_\eta(t) \right\rangle = \sum_{k\sigma} \int dt_1 \left[G_{\text{QD},\sigma\sigma}^R(t, t_1) \Sigma_{\eta,k\sigma\sigma}^{<} + G_{\text{QD},\sigma\sigma}^{<}(t, t_1) \Sigma_{\eta,k\sigma\sigma}^A \right],$$

so that

$$2 \left\langle \hat{I}_\eta(t) \right\rangle \left\langle \hat{I}_{\eta'}(t') \right\rangle = 2 \frac{e^2}{\hbar} \sum_{kk'\sigma\sigma'} |t_{k\sigma}|^2 |t_{k'\sigma'}|^2 \left[F_{\eta,k\sigma}(t, t) + F_{\eta,k\sigma}^*(t, t) \right] \left[F_{\eta',k'\sigma'}(t', t') + F_{\eta',k'\sigma'}^*(t', t') \right], \quad (\text{B25})$$

hence we can obtain

$$\left\langle \left\{ \hat{I}_\eta(t), \hat{I}_{\eta'}(t') \right\} \right\rangle_{\text{disc}} = 2 \left\langle \hat{I}_\eta(t) \right\rangle \left\langle \hat{I}_{\eta'}(t') \right\rangle. \quad (\text{B26})$$

The shot noise is now reduced to

$$\begin{aligned}
S_{\eta\eta'}(t, t') &= \left\langle \left\{ \hat{I}_\eta(t), \hat{I}_{\eta'}(t') \right\} \right\rangle_{\text{conn}} \\
&= \frac{e^2}{\hbar} \sum_{kk', \sigma\sigma'} \left\{ t_{k\sigma} t_{k'\sigma'} G_{1, \text{conn}}^{(2)>}(t, t') - t_{k\sigma} t_{k'\sigma'}^* G_{2, \text{conn}}^{(2)>}(t, t') - t_{k\sigma}^* t_{k'\sigma'} G_{3, \text{conn}}^{(2)>}(t, t') + t_{k\sigma}^* t_{k'\sigma'}^* G_{4, \text{conn}}^{(2)>}(t, t') \right\} + \text{H.C.} \\
&= \frac{e^2}{\hbar} \sum_{k, \sigma} |t_{k\sigma}|^2 \delta_{\eta, \eta'} [G_{\eta, k\sigma\sigma}(t', t) G_{\text{QD}, \sigma\sigma}(t, t') + G_{\eta, k\sigma\sigma}(t, t') G_{\text{QD}, \sigma\sigma}(t', t)]^> \\
&\quad - \frac{e^2}{\hbar} \sum_{kk', \sigma\sigma'} |t_{k\sigma}|^2 |t_{k'\sigma'}|^2 \left\{ \left[\int dt_1 G_{\text{QD}, \sigma'\sigma}(t', t_1) G_{\eta, k\sigma\sigma}(t_1, t) \int dt_2 G_{\text{QD}, \sigma\sigma'}(t, t_2) G_{\eta', k'\sigma'\sigma'}(t_2, t') \right]^> \right. \\
&\quad - \left[G_{\text{QD}, \sigma'\sigma}(t, t') \int \int dt_1 dt_2 G_{\eta, k\sigma\sigma}(t_1, t) G_{\text{QD}, \sigma\sigma'}(t_2, t_1) G_{\eta', k'\sigma'\sigma'}(t', t_2) \right]^> \\
&\quad - \left[G_{\text{QD}, \sigma'\sigma}(t', t) \int \int dt_1 dt_2 G_{\eta, k\sigma\sigma}(t, t_1) G_{\text{QD}, \sigma\sigma'}(t_1, t_2) G_{\eta', k'\sigma'\sigma'}(t_2, t') \right]^> \\
&\quad \left. + \left[\int dt_1 G_{\text{QD}, \sigma'\sigma}(t_1, t') G_{\eta, k\sigma\sigma}(t, t_1) \int dt_2 G_{\text{QD}, \sigma\sigma'}(t_2, t) G_{\eta', k'\sigma'\sigma'}(t', t_2) \right]^> \right\} + \text{H.C.} \\
&= \frac{e^2}{\hbar} \text{Tr} \left\{ \delta_{\eta, \eta'} (\Sigma_\eta^>(t', t) \tilde{\sigma}_z G_{\text{QD}}^<(t, t') \tilde{\sigma}_z + G_{\text{QD}}^>(t', t) \tilde{\sigma}_z \Sigma_\eta^<(t, t') \tilde{\sigma}_z) \right. \\
&\quad - \left[\int dt_1 G_{\text{QD}}(t', t_1) \Sigma_\eta(t_1, t) \right]^> \tilde{\sigma}_z \left[\int dt_2 G_{\text{QD}}(t, t_2) \Sigma_{\eta'}(t_2, t') \right]^< \tilde{\sigma}_z \\
&\quad - \left[\int dt_1 G_{\text{QD}}(t, t') \right]^> \tilde{\sigma}_z \left[\int \int dt_1 dt_2 \Sigma_\eta(t_1, t) G_{\text{QD}}(t_2, t_1) \Sigma_{\eta'}(t', t_2) \right]^< \tilde{\sigma}_z \\
&\quad - \left[\int \int dt_1 dt_2 \Sigma_\eta(t, t_1) G_{\text{QD}}(t_1, t_2) \Sigma_{\eta'}(t_2, t') \right]^> \tilde{\sigma}_z \left[\int dt_1 G_{\text{QD}}(t', t) \right]^< \tilde{\sigma}_z \\
&\quad \left. + \left[\int dt_1 G_{\text{QD}}(t_1, t') \Sigma_\eta(t, t_1) \right]^> \tilde{\sigma}_z \left[\int dt_2 G_{\text{QD}}(t_2, t) \Sigma_{\eta'}(t', t_2) \right]^< \tilde{\sigma}_z, \right. \tag{B27}
\end{aligned}$$

where G_{QD} is the 4×4 matrix form of the elements $G_{\text{QD}, \sigma'\sigma}$. and Σ_η is the 4×4 matrix form of the elements $\Sigma_{\eta, \sigma\sigma} = \sum_k |t_{k\sigma}|^2 G_{\eta, k\sigma\sigma}$. The matrix $\tilde{\sigma}_z = \text{diag}(1, -1, 1, -1)$ describes the different charge of electrons and holes. Finally, we apply the convolution property of Fourier transform $\int_{-\infty}^{\infty} d(t-t') e^{i\omega'(t-t')} x(t-t') y(t'-t) = \frac{1}{2\pi} \int_{-\infty}^{\infty} d\omega F[x](\omega) F[y](\omega + \omega')$ to the above shot noise and obtain

$$\begin{aligned}
S_{\eta\eta'}(\omega') &= \int_{-\infty}^{\infty} d(t-t') e^{i\omega'(t-t')} S_{\eta\eta'}(t-t') \\
&= \frac{e^2}{\hbar} \int_{-\infty}^{\infty} d\omega \text{Tr} \{ \delta_{\eta, \eta'} (\Sigma_\eta^>(\omega) \tilde{\sigma}_z G_{\text{QD}}^<(\omega + \omega') \tilde{\sigma}_z + G_{\text{QD}}^>(\omega) \tilde{\sigma}_z \Sigma_\eta^<(\omega + \omega') \tilde{\sigma}_z) \\
&\quad - [G_{\text{QD}}(\omega) \Sigma_{\eta'}(\omega)]^> \tilde{\sigma}_z [G_{\text{QD}}(\omega + \omega') \Sigma_\eta(\omega + \omega')]^< \tilde{\sigma}_z - [\Sigma_\eta(\omega) G_{\text{QD}}(\omega)]^> \tilde{\sigma}_z [\Sigma_{\eta'}(\omega + \omega') G_{\text{QD}}(\omega + \omega')]^< \tilde{\sigma}_z \\
&\quad + G_{\text{QD}}^>(\omega) \tilde{\sigma}_z [\Sigma_{\eta'}(\omega + \omega') G_{\text{QD}}(\omega + \omega') \Sigma_\eta(\omega + \omega')]^< \tilde{\sigma}_z + [\Sigma_\eta(\omega) G_{\text{QD}}(\omega) \Sigma_{\eta'}(\omega)]^> \tilde{\sigma}_z G_{\text{QD}}^<(\omega + \omega') \tilde{\sigma}_z \}. \tag{B28}
\end{aligned}$$

-
- [1] R. M. Lutchyn, J. D. Sau, and S. Das Sarma, Phys. Rev. Lett. **105**, 077001 (2010).
[2] Y. Oreg, G. Refael, and F. von Oppen, Phys. Rev. Lett. **105**, 177002 (2010).
[3] S. D. Sarma, M. Freedman, and C. Nayak, npj Quantum

- Information **1**, 15001 (2015).
[4] L. Fu and C. L. Kane, Phys. Rev. Lett. **100**, 096407 (2008).
[5] A. C. Potter and P. A. Lee, Phys. Rev. Lett. **105**, 227003 (2010).

- [6] A. Y. Kitaev, *Physics-Uspekhi* **44**, 131 (2001).
- [7] C. J. Bolech and E. Demler, *Phys. Rev. Lett.* **98**, 237002 (2007).
- [8] F. Pientka, G. Kells, A. Romito, P. W. Brouwer, and F. von Oppen, *Phys. Rev. Lett.* **109**, 227006 (2012).
- [9] D. E. Liu and H. U. Baranger, *Phys. Rev. B* **84**, 201308 (2011).
- [10] A. R. Akhmerov, J. Nilsson, and C. W. J. Beenakker, *Phys. Rev. Lett.* **102**, 216404 (2009).
- [11] L. Fu and C. L. Kane, *Phys. Rev. Lett.* **102**, 216403 (2009).
- [12] J. Danon, A. B. Hellenes, E. B. Hansen, L. Casparis, A. P. Higginbotham, and K. Flensberg, *Phys. Rev. Lett.* **124**, 036801 (2020).
- [13] A. Haim, E. Berg, F. von Oppen, and Y. Oreg, *Phys. Rev. Lett.* **114**, 166406 (2015).
- [14] L. Fidkowski, J. Alicea, N. H. Lindner, R. M. Lutchyn, and M. P. A. Fisher, *Phys. Rev. B* **85**, 245121 (2012).
- [15] B. H. Wu and J. C. Cao, *Phys. Rev. B* **85**, 085415 (2012).
- [16] T. Jonckheere, J. Rech, A. Zazunov, R. Egger, A. L. Yeyati, and T. Martin, *Phys. Rev. Lett.* **122**, 097003 (2019).
- [17] K. Flensberg, *Phys. Rev. B* **82**, 180516 (2010).
- [18] K. T. Law, P. A. Lee, and T. K. Ng, *Phys. Rev. Lett.* **103**, 237001 (2009).
- [19] J. J. He, T. K. Ng, P. A. Lee, and K. T. Law, *Phys. Rev. Lett.* **112**, 037001 (2014).
- [20] D. Bagrets and A. Altland, *Phys. Rev. Lett.* **109**, 227005 (2012).
- [21] Y. Peng, F. Pientka, Y. Vinkler-Aviv, L. I. Glazman, and F. von Oppen, *Phys. Rev. Lett.* **115**, 266804 (2015).
- [22] J. Liu, A. C. Potter, K. T. Law, and P. A. Lee, *Phys. Rev. Lett.* **109**, 267002 (2012).
- [23] O. A. Awoga, J. Cayao, and A. M. Black-Schaffer, *Phys. Rev. Lett.* **123**, 117001 (2019).
- [24] G. Sharma and S. Tewari, *Phys. Rev. B* **93**, 195161 (2016).
- [25] J. Cayao, E. Prada, P. San-Jose, and R. Aguado, *Phys. Rev. B* **91**, 024514 (2015).
- [26] S. Nadj-Perge, I. K. Drozdov, J. Li, H. Chen, S. Jeon, J. Seo, A. H. MacDonald, B. A. Bernevig, and A. Yazdani, *Science* **346**, 602 (2014).
- [27] V. Mourik, K. Zuo, S. M. Frolov, S. Plissard, E. P. Bakkers, and L. P. Kouwenhoven, *Science* **336**, 1003 (2012).
- [28] A. Das, Y. Ronen, Y. Most, Y. Oreg, M. Heiblum, and H. Shtrikman, *Nature Physics* **8**, 887 (2012).
- [29] S. Zhu, L. Kong, L. Cao, H. Chen, M. Papaj, S. Du, Y. Xing, W. Liu, D. Wang, C. Shen, F. Yang, J. Schneeloch, R. Zhong, G. Gu, L. Fu, Y.-Y. Zhang, H. Ding, and H.-J. Gao, *Science* **367**, 189 (2020).
- [30] H.-H. Sun, K.-W. Zhang, L.-H. Hu, C. Li, G.-Y. Wang, H.-Y. Ma, Z.-A. Xu, C.-L. Gao, D.-D. Guan, Y.-Y. Li, C. Liu, D. Qian, Y. Zhou, L. Fu, S.-C. Li, F.-C. Zhang, and J.-F. Jia, *Phys. Rev. Lett.* **116**, 257003 (2016).
- [31] S. Frolov, (2021), 10.1038/d41586-021-00954-8.
- [32] J. Nilsson, A. R. Akhmerov, and C. W. J. Beenakker, *Phys. Rev. Lett.* **101**, 120403 (2008).
- [33] K. M. Tripathi, S. Das, and S. Rao, *Phys. Rev. Lett.* **116**, 166401 (2016).
- [34] D. E. Liu, M. Cheng, and R. M. Lutchyn, *Phys. Rev. B* **91**, 081405 (2015).
- [35] A. Golub and B. Horovitz, *Phys. Rev. B* **83**, 153415 (2011).
- [36] D. Giuliano, S. Paganelli, and L. Lepori, *Phys. Rev. B* **97**, 155113 (2018).
- [37] S. Smirnov, *Phys. Rev. B* **99**, 165427 (2019).
- [38] S. Smirnov, *New Journal of Physics* **19**, 063020 (2017).
- [39] D. Beckmann, H. B. Weber, and H. v. Löhneysen, *Phys. Rev. Lett.* **93**, 197003 (2004).
- [40] S.-B. Zhang and B. Trauzettel, *Phys. Rev. Lett.* **122**, 257701 (2019).
- [41] A. Cottet, W. Belzig, and C. Bruder, *Phys. Rev. Lett.* **92**, 206801 (2004).
- [42] Y. Zhu, W. Li, T.-h. Lin, and Q.-f. Sun, *Phys. Rev. B* **66**, 134507 (2002).
- [43] X. Cao, Y. Shi, X. Song, S. Zhou, and H. Chen, *Phys. Rev. B* **70**, 235341 (2004).
- [44] Y. Zhu, Q.-f. Sun, and T.-h. Lin, *Phys. Rev. B* **65**, 024516 (2001).
- [45] Q.-f. Sun, J. Wang, and T.-h. Lin, *Phys. Rev. B* **59**, 3831 (1999).
- [46] Q.-f. Sun, J. Wang, and T.-h. Lin, *Phys. Rev. B* **62**, 648 (2000).
- [47] F. M. Souza, A. P. Jauho, and J. C. Egues, *Phys. Rev. B* **78**, 155303 (2008).
- [48] B. Van Heck, A. Akhmerov, F. Hassler, M. Burrello, and C. Beenakker, *New Journal of Physics* **14**, 035019 (2012).
- [49] T. Karzig, Y. Oreg, G. Refael, and M. H. Freedman, *Phys. Rev. X* **6**, 031019 (2016).
- [50] J. C. Cuevas, A. Martín-Rodero, and A. L. Yeyati, *Phys. Rev. B* **54**, 7366 (1996).
- [51] A. Zazunov, R. Egger, and A. Levy Yeyati, *Phys. Rev. B* **94**, 014502 (2016).
- [52] L. Xu, X.-Q. Li, and Q.-F. Sun, *Journal of Physics: Condensed Matter* **29**, 195301 (2017).
- [53] Y. Meir and N. S. Wingreen, *Phys. Rev. Lett.* **68**, 2512 (1992).
- [54] H. Haug, A.-P. Jauho, *et al.*, *Quantum kinetics in transport and optics of semiconductors*, Vol. 2 (Springer, 2008) Chap. 4 and 12.
- [55] Z. Y. Zeng, B. Li, and F. Claro, *Phys. Rev. B* **68**, 115319 (2003).
- [56] L. V. Keldysh *et al.*, *Sov. Phys. JETP* **20**, 1018 (1965).
- [57] L. Fu and C. L. Kane, *Phys. Rev. B* **79**, 161408 (2009).
- [58] Y. Blanter and M. Büttiker, *Physics Reports* **336**, 1 (2000).
- [59] R. Cron, M. F. Goffman, D. Esteve, and C. Urbina, *Phys. Rev. Lett.* **86**, 4104 (2001).
- [60] J. C. Cuevas, A. Martín-Rodero, and A. L. Yeyati, *Phys. Rev. Lett.* **82**, 4086 (1999).
- [61] M. J. M. de Jong and C. W. J. Beenakker, *Phys. Rev. B* **49**, 16070 (1994).